

## Application of nanofluids in solar cooling system: Dynamic simulation by means of TRNSYS software

Bernardo Buonomo<sup>1</sup>, Furio Cascetta<sup>1</sup>, Luca Cirillo<sup>1\*</sup>, Sergio Nardini<sup>1,2</sup>

<sup>1</sup> Dipartimento di Ingegneria, Università degli Studi della Campania “L. Vanvitelli”, Real Casa dell’Annunziata, Via Roma 29, Aversa (POSTAL CODE), Italy

<sup>2</sup> Sun Energy Europe S.r.l., Academic Spin-Off, Via B. De Capua 26, Capua (CE) 81043, Italy

Corresponding Author Email: [luca.cirillo@unicampania.it](mailto:luca.cirillo@unicampania.it)

[https://doi.org/10.18280/mmc\\_b.870305](https://doi.org/10.18280/mmc_b.870305)

**Received:** 8 March 2018

**Accepted:** 20 April 2018

### Keywords:

solar cooling, nanofluids, transient simulation, renewable energy, energy management

## ABSTRACT

Convective heat transfer can be enhanced passively by using fluids with high value of the thermal conductivity. An innovative method of enhancement of thermal conductivity of base fluids is to insert nanoparticles. In recent years, nanofluids and their possible applications have been extensively studied.

In this study, simulation based on a performance analysis of a solar cooling system is carried out by means of TRNSYS. First the analysis determines the peak energy demand for a building located in Naples. Beside, for the same configuration of solar system both pure water and Al<sub>2</sub>O<sub>3</sub>/water based nanofluids are considered as working fluids. Different values of volume nanoparticles concentrations, equal to 3%, and 6%, are investigated. The configuration is fully modelled in TRNSYS and dynamic simulations are run for the entire year. Various performance factors such as useful energy gain from collector, solar fraction, primary energy savings and pumping consumption are evaluated. Simulations results demonstrate that for the whole summer season, using nanofluids as working fluid, always higher primary energy savings results. Besides, solar fraction, difference between nanofluids with nanoparticles concentration of 3% and 6% is estimated to be marginal. In terms of PEC and primary energy savings, nanofluids with nanoparticles concentration of 6% has presented higher values.

## 1. INTRODUCTION

An interesting solution for air conditioning in summer time is a solar cooling system. In recent years SC (Solar cooling) system has largely developed to meet the high demand of energy for cooling and higher comfort standards in buildings. The emissions of CO<sub>2</sub>, which grows with the production of energy from fossil fuels and the use of climate-altering cooling working fluids. The aim of many studies on SC system is to improve the useful energy gain form collector and reduce the auxiliary energy and other parasitic energy losses from electrical devices [1-4]. A way to improve the heat transfer of conventional fluids is to suspend in them small solid metallic, non-metallic or polymeric nanoparticles [5]. Thermal properties of nanofluids in solar collector is studied by many authors. Muhammad et al. [6] carried out a review on thermal performance enhancement of flat plate and evacuate tube solar collectors using nanofluids. They reviewed recent progress and applications of nanofluids and discussed the impact of nanoparticles in solar collector on economic and environmental viewpoints. Lu at al. [7] have studied the thermal performance of an open thermosiphon using water based CuO nanofluids for high-temperature evacuated solar collectors. In their experimental analysis the results show that using water based CuO nanofluids, the thermal performance of the open thermosiphon increase with increase of the operating temperature. Finally, they have observed that the thermal performance of the evaporator and evaporating heat transfer coefficients increase by about 30% compared with those of water. Other interesting review on the applications of

nanofluids in solar energy field is developed by Khanafer and Vafai [8]. Their review is structured in three different parts: the first part focuses on the latest results about thermal conductivity, viscosity, specific heat and thermal expansion coefficient reported in literature; the second part focuses on the applications of nanofluids in different solar systems as solar collectors, photovoltaic systems, thermal energy storage systems; in the third part, they discussed about the challenges and the bio-engineering safety concerns of using nanofluids. Analytical and numerical investigations are carried to evaluate the thermal performance [9-13]. Kasaiean et al. [9] in their work consider nanofluid as the heat transfer medium. They used a finite difference scheme (FDM) and create a MATLAB code to investigate the thermal performance of a heat collecting element (HCE). Their results show the radiant loss increased from 26.5 to 57.3 W/m in the range of 30-100°C. The convective heat transfer coefficient increased by adding multiwall carbon nanotube (MWCNT) nanoparticles to the base fluid (thermal oil). The improvement is 15% by adding 6% volume fraction of nanoparticles. In the work of Bianco et al. [10] a numerical analysis of the Al<sub>2</sub>O<sub>3</sub> water nanofluid for application in flat plate PV/T is accomplished. They fixed a numerical model by means COMSOL and simulated two dimensional nanofluids laminar convection flows for Re comprised between 250 and 1000, concentration between 0% and 6%, particles dimension of 20 and 40 nm in an asymmetric heated channel. Their results show that nanofluids permits better cooling performances. Besides, Nusselt number and average heat transfer coefficient for nanofluids increase in a range of 2% and 15%. On the other hand, the pressure drop

increases in substantial way. A numerical investigation and experimental validation is carried out by Hawwash et al. [11]. Their work focused on performance of a flat plate solar collector (FPSC) with different types of working fluid: water, alumina nanofluids with six different volume fractions in the range 0.1%-3%. The experimental validation was carried out in Egypt, their result show that using alumina nanofluid improves the collector thermal efficiency compared to water by about 3 and 18% at low and high temperature differences. The numerical results shown that increasing the percentage of alumina nanofluid increases the thermal efficiency of the FPSC until 0.5% volume fraction, and further increase has a negative effect on the thermal performance and the pressure drop increases with increasing the volume fractions of nanofluid. Genc et al. [12] evaluated the thermal performance of a nanofluid-based flat plate solar collector. The analysis carried out considering different working fluids such as water and three different volumetric concentrations of Al<sub>2</sub>O<sub>3</sub> nanoparticles as 1%, 2% and 3% to demonstrate the effect at different flow Reynolds numbers. Their results indicate that the maximum increase of the outlet temperature is obtained by 7.20% at 0.004 kg/s and 3%(vol.) mass flow rate and volumetric concentration, respectively, in July. Other interesting results is the highest efficiency is obtained as 83.90% at 0.06 kg/s mass flow rate for 1%(vol.) in October. Besides nanofluid is more effective on the collector efficiency at below 0.016 kg/s. Many experimental investigations carried out to evaluate properties of solar collectors with nanofluids such as efficiency, thermal conductivity and heat transfer coefficient [13-15]. Ozsoy and Corumlu [13] carried out an experimental analysis to evaluate thermal efficiency of a thermosiphon heat pipe evacuated tube solar collector using silver-water nanofluid for commercial applications. They noted that nanofluid working fluid increased the efficiency of solar collector between 20.7% and 40% compared with the pure water. An experimental test of an innovative high concentration nanofluid solar collector is accomplished by Colangelo et al. [14]. They used a modified flat panel solar thermal collector with two different working fluids: distilled water and Al<sub>2</sub>O<sub>3</sub>-water based nanofluid 3%(vol.). Their experimental results shown that an increase of thermal efficiency up to 11.7% compared to that measured with water has been obtained by using nanofluids. Other interesting result is that the effect of nanofluid on thermal efficiency is greater at high temperatures. Farajzadeh et al. [15] carried out experimental and numerical investigations on the effect of Al<sub>2</sub>O<sub>3</sub>/TiO<sub>2</sub>-water based nanofluids on thermal efficiency of the flat plate solar collector. They considered three different volume rates: 1.5 l/m, 2.0 l/m and 2.5 l/m. The results show that the thermal efficiency enhances about 19%, 21% and 26% by using Al<sub>2</sub>O<sub>3</sub> (0.1% vol.), TiO<sub>2</sub> (0.1% vol.) and the mixture of these two nanofluids, respectively. Besides, by increasing the volumetric concentration of the nanofluid mixture from 0.1% to 0.2% results 5% improvement in the thermal efficiency of the solar collector.

The objective of this work is to model and simulate a complete solar cooling system made up evacuated tube (ETC) solar collectors, thermal storage tank and LiBr-H<sub>2</sub>O based single effect absorption chiller. Two different working fluids are considered: pure water and Al<sub>2</sub>O<sub>3</sub>-water with two different volumetric nanoparticles concentrations, 3% and 6%. A transient analysis by means of TRNSYS is accomplished to meet the cooling energy demand by means of a typical plant of SCS (solar cooling system) with nanofluids. The results are

presented in terms of useful energy gain from collectors, solar fraction, primary energy saving and significant plant temperatures.

## 2. SYSTEM CONFIGURATION

The SCS configuration is such as to meet the energy cooling demand of an office building in Naples, Fig.1. The ETSCs (evacuated thermal solar collector), a storage tank, a hydraulic pump and a controller are considered for the hot loop. The hot fluid flows into the collectors and reaches a hot storage tank at high temperature T<sub>coll,o</sub>. The working fluid is sent back to the collectors by means of a pump when the outlet water from hot storage tank, T<sub>st,o</sub>, is lower than 90°C. The ETSCs work isolated from the chiller and the circulation in the first part of the system continues until the water inside the storage tank reaches the required working temperature. In this work, nanofluids are considered as the working fluid (Al<sub>2</sub>O<sub>3</sub>) for the hot loop. Physical properties of the Al<sub>2</sub>O<sub>3</sub> nanoparticles and water in the calculations are presented in Table 1. Nanofluid thermal conductivity, specific heat capacity, density and dynamic viscosity are evaluated with Eqs. (1-4).

**Table 1.** Physical properties of nanomaterial and water

Nanoparticles	$\rho$ (kg/m <sup>3</sup> )	k (W/mK)	c <sub>p</sub> (J/kgK)
Al <sub>2</sub> O <sub>3</sub>	3970	36	773
Water	997	0.605	4178

Thermal conductivity of nanofluids is evaluated by the following equation [16-17]:

$$\frac{k_{nf}}{k_{bf}} = \frac{\frac{k_p}{k_{bf}} + 5 - 5\left(1 - \frac{k_p}{k_{bf}}\right)\phi}{\frac{k_p}{k_{bf}} + 5 + \left(1 - \frac{k_p}{k_{bf}}\right)\phi} \quad (1)$$

Several correlations for specific heat capacity are available but the below formula, presented by Xuan and Roetzel [18], presents the lowest error:

$$c_{pnf} = \frac{\phi\rho_p c_{pp} + (1-\phi)\rho_{bf} c_{pbf}}{\rho_{nf}} \quad (2)$$

The density is evaluated by means (Kasaeian et al. [19]):

$$\rho_{nf} = \rho_p\phi - \rho_{bf}(1-\phi) \quad (3)$$

The Einstein's equation [20] could be used for calculating the dynamic viscosity of the nanofluid:

$$\mu_{nf} = (1 + 2.5\phi)\mu_{bf} \quad (4)$$

The single effect absorption chiller, receives the hot fluid from the hot storage tank at 90°C (the required input temperature). When T<sub>st,o</sub> is less than the temperature required by chiller, the supplementary boiler inside the storage tank will be activated thus the set-point temperature of inlet hot water

of chiller is guaranteed when the solar radiation is low. For this reason, a thermostat is installed. The chiller, in addition, has a connection both with the cooling tower and with a cold storage tank, which acts as a fly-wheel with the fan coils.

### 3. MODELING IN TRNSYS

The described solar system, based on a single effect absorption chiller (15 kW of power), is fully modelled in TRNSYS (version 17), with weather data of Naples ( $40^{\circ}51'22''N; 14^{\circ}14'47''E$ ) as the reference climate data. The aim of this work is to study the effect of the system configuration and the overall thermal performance. The effects of boiling and cooling of the working fluid and the pressure drops inside the pipes and valves are not considered in the analysis. In view of the above assumptions, the predicted values of various performance factors are larger than in magnitudes than in a real system. The scheme of the considered solar cooling system in TRNSYS is shown in Fig. 2.

#### 3.1 Solar collector

In this study ETSCs (Type 71) are considered. The investigation is carried out with three different nanoparticles volume concentration of the working nanofluids (i.e. 0%, 3% and 6%) with volume flow rate equal to 0.47 l/s. The thermal efficiency is calculated by equations presented in Ghaderian and Sidik [21], in particular:

Water

$$\eta = 0.2412 - 1.3648 \frac{\Delta T}{G} \quad (5)$$

$Al_2O_3$ -water 3% vol.

$$\eta = 0.4477 - 1.7180 \frac{\Delta T}{G} \quad (6)$$

$Al_2O_3$ -water 6% vol.

$$\eta = 0.5697 - 2.0186 \frac{\Delta T}{G} \quad (7)$$

They investigated the effects of using  $Al_2O_3$ /distilled water nanofluid as the working fluid on the thermal efficiency defining the equations (5-7). They used dimensions and proportions of ETSC shown in Table 2. In this work, the same solar collector is considered but with a total absorbing area of  $100 m^2$ .

#### 3.2 Storage tanks

In this study, a hot storage tank and a cold storage tank are considered with volume equal to  $5 m^3$  and  $2 m^3$ , respectively. To define the tanks, type 4a is used by considering a stratified storage tank with uniform losses and with multi-node approach in which the tank is divided into N nodes. Each node is governed by the tank energy balance as a function of time. The flow (water) is drawn to supply the chiller (must be the highest node of the tank) and the return flow is conveyed towards the lower node of the tank. In this study, the hot storage tank is divided into 6 nodes, while the cold storage

tank presents 1 node. Both tanks have a constant heat loss coefficient of  $0.69 W/m^2K$ . In addition, the hot tank is equipped with an auxiliary boiler: an integrated boiler that is activated when the temperature of the fluid falls below the set point temperature.

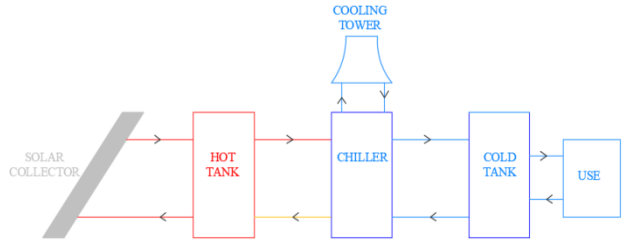


Figure 1. 1-D model of solar cooling system

Whenever boiler is on, the heat energy ( $Q_{boiler}$ ) required to increase the temperature of the working fluid from inlet temperature ( $T_{st,in}$ ) to the desired outlet temperature ( $T_{st,o}$ ) is calculated as:

$$\dot{Q}_{boiler} = m_w c_{p,w} (T_{st,o} - T_{st,in}) \quad (8)$$

where  $m_w$  and  $c_{p,w}$  are the mass flow rate and specific heat of water, respectively.

#### 3.3 Absorption chiller

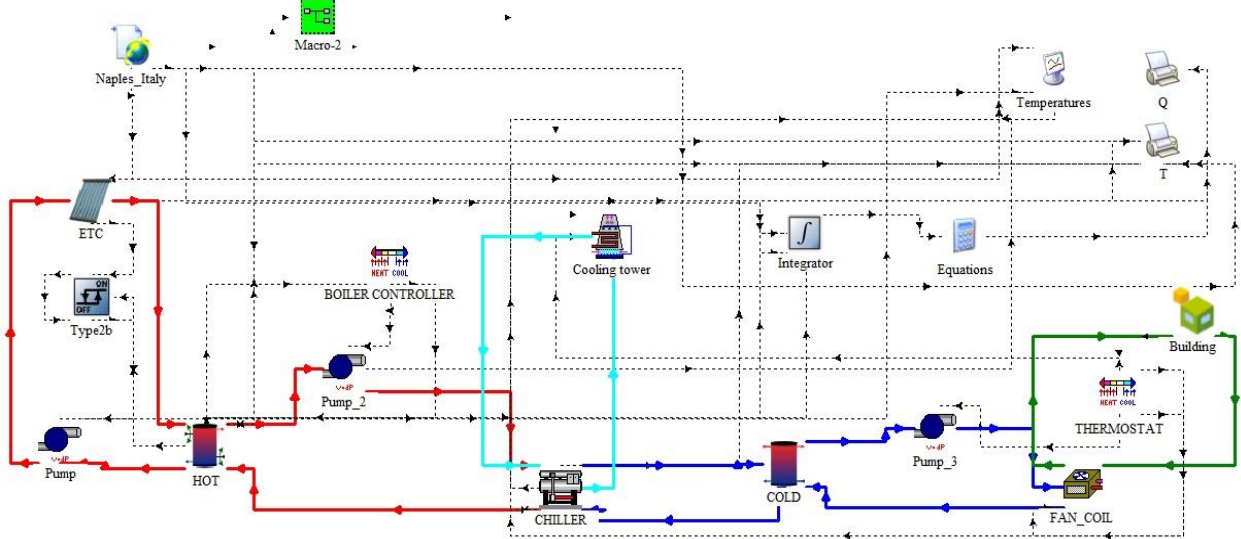
Type 107 is used to model the absorption chiller thermally powered by hot water from storage tank to regenerate the absorbed refrigerant in the generator from the solution of refrigerant-absorbent mixture. In this case the absorption machine has a rated capacity of 15 kW with a rated COP of 0.71 kW.

Table 2. Specification of ETSC

Specification	Unit	Dimension
Gross area	$m^2$	2.57
Aperture area	$m^2$	2.22
Absorber area	$m^2$	2.36
Length	in	70.8"
Width/width incl. connection	mm	1560/1612
Max operating pressure	bar	10
Absorber	-	Aluminum
Absorption ( $\alpha$ )/emission ( $\epsilon$ )	-	0.96/0.06
Collector housing	-	Aluminum
Collector glazing	-	Evacuated tubes
Number of tubes	-	18
Outer glass tube diameter	in	2.28"
Inner glass tube diameter	in	1.85"
Sealing material	-	Silicone
Frame material	-	Stainless steel

#### 3.4 Building load variation

The SCS has designed to meet cooling energy demand of an office building of  $250 m^2$ , with  $37 m^2$  of windows (almost 15%). A 1-D simple scheme of plant is shown in Fig. 1. The office schedule is from 8:00 to 18:00 and it is considered as a single thermal zone.



**Figure 2.** Solar cooling system scheme in TRNSYS

Type 56 is used in this study to model the office building. The 3-D sample building was developed using the graphical tool SketchUp [22], and later imported to TRNSYS, where the profiles of occupation of the building and the physical properties of the materials of the walls and windows were added. Thus, by simulating this building model, it is generated a typical seasonal cooling demand on an hourly timescale. The monthly values of the demand are presented in Fig.3. Table 3 summarizes all types used in TRNSYS.

### 3.5 Weather data

Climatic data is defined by type 99 containing user defined notepad file of Naples's weather data having latitude and longitude of  $40.51^{\circ}\text{N}$  and  $14.16^{\circ}\text{E}$ , respectively. Figure 4 shows the variation of the ambient temperature for the whole year, where the maximum temperature is in the range of  $30\text{--}35^{\circ}\text{C}$  in summer months.

**Table 3.** Trnsys components

Component	Type
ETCs	71
Hot storage tank	4a
Cold storage tank	4a
Pumps	740
Absorption chiller	107
Solar collector controller	2b
Boiler controller/Termostat	108
Cooling tower	510
Fan coil	600
Building	56

## 4. PERFORMANCE FACTORS

The performance factors for performance evaluation and comparison different working fluids are defined as follow:

### 4.1.1 Solar fraction

Solar fraction is the ratio between the energy from the solar system and the total energy required by the plant. It can vary between 0 and 1, it means that the system works completely

powered by the boiler or completely powered by the solar collectors, respectively. The aim of a SCS is to reach a SF  $\sim 1$ . Solar fraction is given by, [23]:

$$SF = \frac{Q_{\text{solar}}}{Q_{\text{solar}} + Q_{\text{boiler}}} \quad (9)$$

where  $Q_{\text{solar}}$  is the solar thermal gain from solar collectors and  $Q_{\text{boiler}}$  is heat of auxiliary boiler. The energy are related to one month.

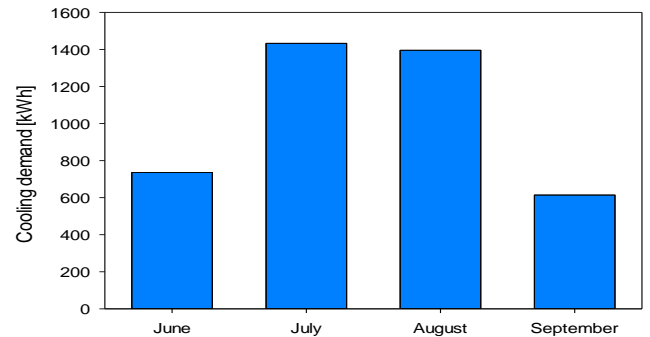


**Figure 3.** Monthly cooling load variation

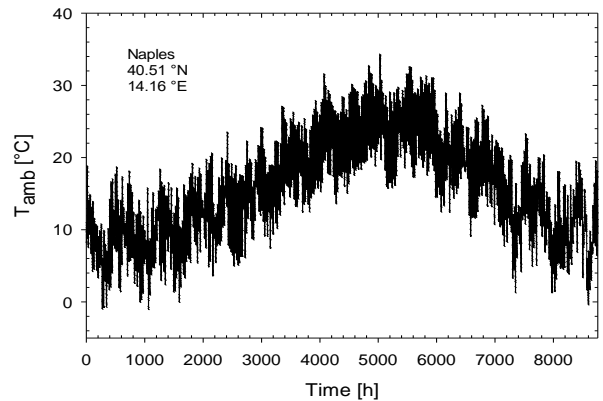


**Figure 4.** Ambient temperature of Naples in the year

#### 4.1.2 Primary energy savings

The primary energy savings is defined by follow equation, [24]:

$$f = 1 - \left[ \frac{\frac{Q_{boiler}}{\varepsilon_{heat}}}{\frac{Q_{cooling,ref}}{COP_{ref} \varepsilon_{electricity}}} \right] \quad (10)$$

where:  $\varepsilon_{heat}$  is the boiler efficiency,  $Q_{cooling,ref}$  is the cooling energy provided by a conventional refrigeration system; COP is the compression chiller efficiency; finally  $\varepsilon_{electricity}$  is the efficiency of a thermal power plant. The term in square brackets represents the ratio between the primary energy consumption by the auxiliary boiler in the SCS and the total primary energy consumption of the conventional refrigerator system to meet the same cooling load. Typical values of conversion factors are assumed as follow:

$\varepsilon_{electricity} = 0.4$  (ration of electricity produced to the fossil primary energy)

$\varepsilon_{heat} = 0.91$  (ratio of useful heat energy to the fossil primary energy)

COP = 2.5 (typical COP of a conventional system)

## 5. RESULTS

Simulations are performed for the whole summer season, i.e. from June to September. The TRNSYS simulation is run with 1-hour time step. The selected system successfully maintains the room temperature below the set point value of 26 °C, even when the ambient temperature is higher than 32 °C during the peak summer season. The SCS presented in this work have no experimental data for validation but the trends of the obtained results have been checked in literature. Figure 5 shows the trend of characteristic temperatures in a typical summer day. It is evident that for pure water the outlet temperature of collector remains below 80°C (set point-temperature of the supplementary boiler). Besides, the use of pure water as working fluid,  $T_{out,coll}$  gives a nearly periodic behavior while by using nanofluids as working fluid all temperatures show nearly a constant trend.

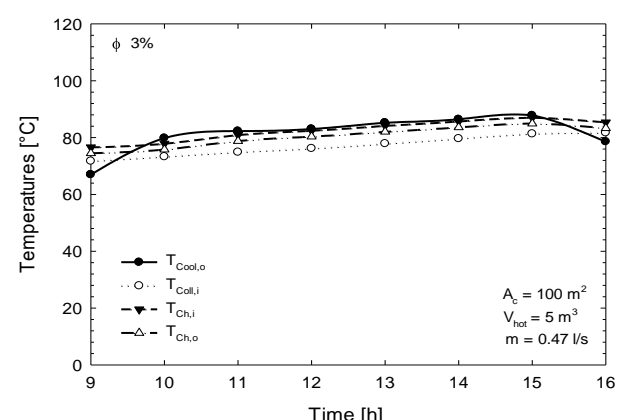
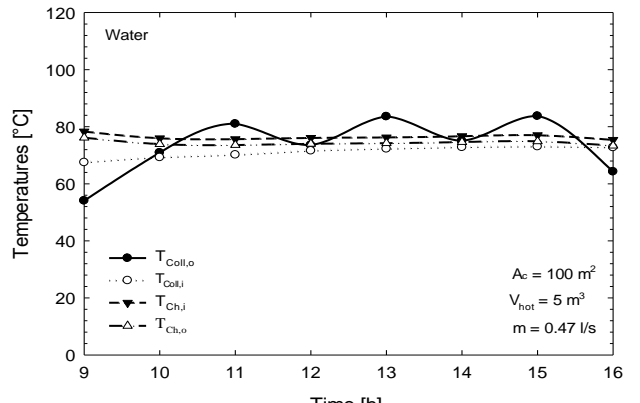
The heat energy rates of the solar collector, auxiliary boiler during cooling season (June-September) is shown in Fig.6. By considering the pure water as working fluid, the supplementary energy ( $Q_{boiler}$ ) is greater than solar thermal gain from collectors ( $Q_{solar}$ ) in the whole summer period. Besides, the energy cooling demand is as high as the difference between  $Q_{solar}$  and  $Q_{boiler}$  high. In fact, in June and September the gap between these two values is relatively minimal. Moreover,  $Q_{solar}$  is higher in June because the cooling demand is low, the storage tank is not affected by the effect of the hot water out from the absorption chiller and the inlet water temperature into solar collectors is higher. Besides, in September,  $Q_{solar}$  and  $Q_{boiler}$  reach a minimum, because the solar irradiation and the cooling demand decreases. By considering the nanofluid ( $\phi=3\%$ ) as the working fluid, it is possible to note that  $Q_{solar}$  is higher than  $Q_{boiler}$  in all the summer season. In the hottest months, even if the absorption machine works more, this fact does not involve a substantial decrease of the temperature in the storage tank. Besides, the inlet temperature of the working fluid into solar collectors

increases, thus the solar thermal gain from solar collectors increases. This phenomenon is accentuated considering the nanofluid with  $\phi=6.0\%$ . In fact, it is noted that in the warmer months the supplementary energy is minimum, so the absorption machine can operate with the only contribution of the solar field.

Monthly variation of solar fraction using different working fluids is shown in Fig.7. The maximum solar fraction is obtained for nanofluid with volumetric concentration  $\phi=6\%$ . It is possible to note that, by considering pure water, the solar fraction decreases during the warmer months because the effects of the outlet hot water temperature from the absorption chiller are strong. The absorption chiller works many times, thus the temperature in the storage tank decreases and the auxiliary boiler remains on for a longer time. Furthermore, the results show that the use of the Al<sub>2</sub>O<sub>3</sub>- water mixture with  $\phi=3\%$  and  $6\%$ , in comparison to simple pure water as working fluid, increased the SF up to 54.6% and 57.4% respectively.

Figure 8 illustrates the monthly fractional primary energy savings,  $f$ . As the auxiliary energy increases primary energy savings decreases and vice-versa. A value of  $f < 0$ , as in the case of pure water, means that the SCS not meet the cooling energy demand during all summer season. Besides, in June and September, despite  $Q_{boiler}$  is lower than other months (because there are few hot days), primary energy consumption of a reference conventional cooling system is higher.

In June, July and August the  $Q_{boiler}$  is higher but also the energy of a conventional cooling system is higher, and for this reason, in the warmer months,  $f$  is higher. To analyze in a better way the effect of nanofluids, a synthetic indicator including both heat transfer rate (useful energy gain from collectors) and pumping energy consumption is to be utilized.



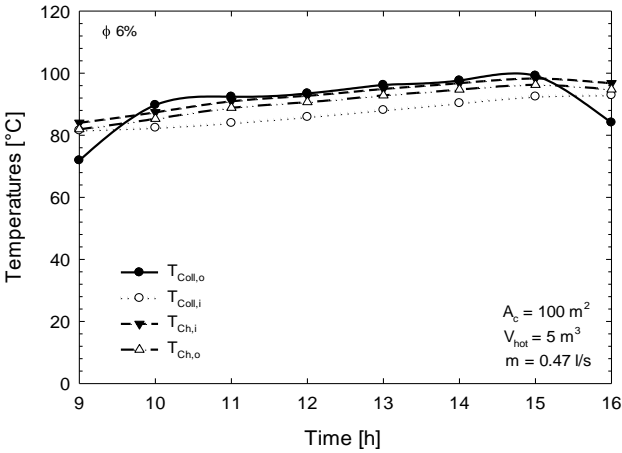


**Figure 5.** Temperature profiles in a typical summer day (30 July)

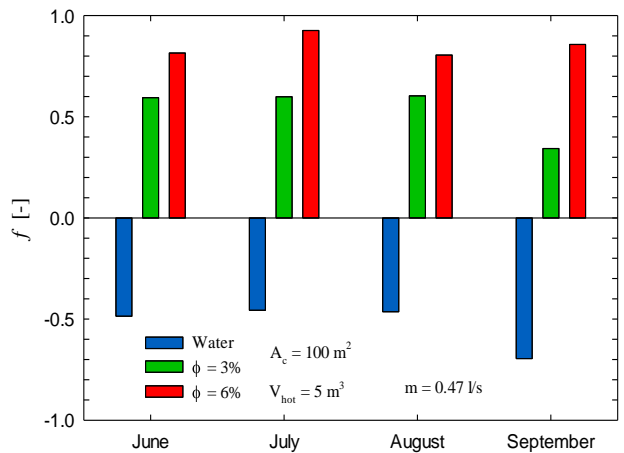


**Figure 8.** Seasonal fractional primary energy savings for different working fluids

According to Roy et al. [25], the performance energy criterion (PEC) is taken into account. PEC is defined according to the following equation:

$$PEC = \frac{\int \dot{Q}_{solar}}{\int \dot{W}} \quad (11)$$

PEC represents the ration between the heat transfer rate,  $\dot{Q}_{solar}$ , and the pumping power  $\dot{W}$ . The analysis of the PEC, Fig. 10, demonstrates that nanofluids represents the best choice for the same volumetric flow in terms of ratio between the energy gain from solar collectors and pumping power.

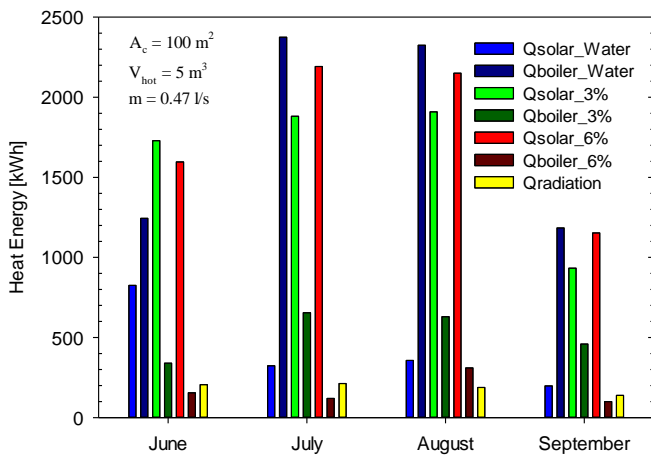


**Figure 6.** Trend of  $Q_{solar}$  and  $Q_{boiler}$  for different working fluids during summer period

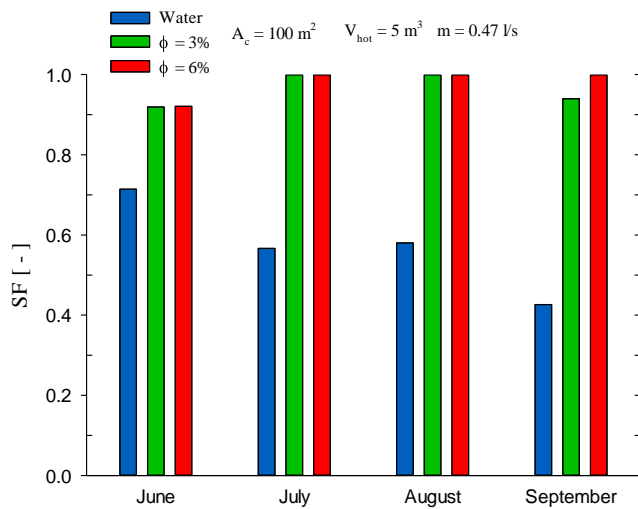


**Figure 7.** Monthly solar fraction for different working fluids during summer period

## 6. CONCLUSIONS

In this work, thermal performance of a solar based single effect absorption cooling system having a peak cooling capacity of 15 kW are investigated by means of a TRNSYS model. In addition, three different working fluids into the ETSC ( $A_c = 100 m^2$ ) are considered: pure distilled water;  $Al_2O_3$ -water nanofluid ( $\phi = 3\%$  and  $6\%$ ).

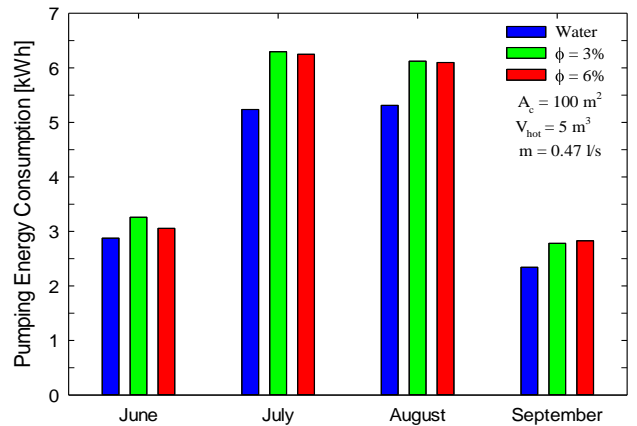


**Figure 9.** Pumping energy consumption during cooling season

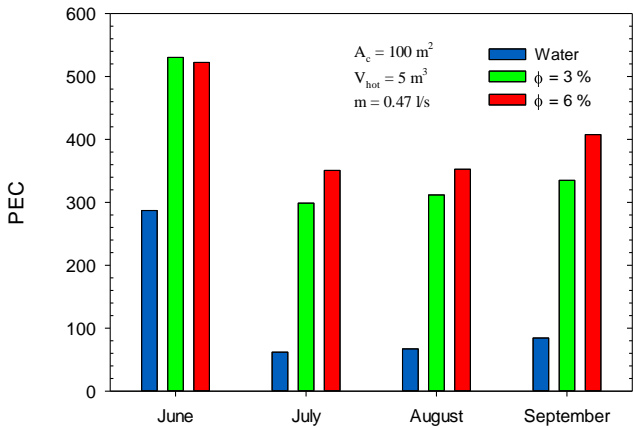


**Figure 10.** Monthly PEC by varying working fluids

Weather data file for the site of Naples ( $40.51^{\circ}\text{N}$ ,  $14.16^{\circ}\text{E}$ ) is used to simulate the system for the entire summer season. The configuration with  $\text{Al}_2\text{O}_3$ -water nanofluid (6%) is the best in terms of solar thermal gain from collectors during warmer months (July-August). In terms of SF, configuration with nanofluids is better for whole cooling season, obtaining SF=1 in July, August, September and July and August for  $\phi=6\%$  and 3%, respectively. Considering the fractional energy savings, configuration with  $\phi=6\%$  offers greater savings than pure water. Finally, the configuration with working fluid the nanofluid of  $\phi=3\%$  presents higher pumping energy consumption than the other two. Compared with pure water, the pumping energy consumption is higher because the viscosity of the fluid is higher. Compared with nanofluid with  $\phi=6\%$ , the pumping energy consumption is higher because the effect of outlet hot water temperature from absorption chiller on temperature of the storage tank is greater, thus the pump remains on for longer. However, the difference is minimum in terms of electricity cost.

## REFERENCES

- [1] Nienborg B, Dalibard A, Schnabel L, Eicker U. (2017). Approaches for the optimized control of solar thermal driven cooling systems. *Applied Energy* 185: 732-44. <https://doi.org/10.1016/j.apenergy.2016.10.106>
- [2] Cirillo L, Della Corte A, Nardini S. (2016). Feasibility study of solar cooling thermally driven system configurations for an office building in Mediterranean area. *International Journal of Heat and Technology* 34(2): 472-80. <https://doi.org/10.18280/ijht.34S240>
- [3] Cascetta F, Cirillo L, Della Corte A, Nardini S. (2017). Comparison between different solar cooling thermally driven system solutions for an office building in Mediterranean Area. *International Journal of Heat and Technology* 35(1): 130-138. <https://doi.org/10.18280/ijht.350118>
- [4] Khan MSA, Badar AW, Talha T, Khan MW, Butt FS. (2018). Configuration based modelling and performance analysis of single effect solar absorption cooling system in TRNSYS. *Energy Conversion and Management* 157: 351-63. <https://doi.org/10.1016/j.enconman.2017.12.024>
- [5] Bianco V, Manca O, Nardini S, Vafai K. (2015). *Heat Transfer Enhancement with Nanofluids*, Publisher CRC, Taylor and Francis Group.
- [6] Muhammad MJ, Muhammad IA, Sidik NAC, Yazid MNAWM. (2016). Thermal performance enhancement of flat-plate and evacuated tube solar collectors using nanofluid: A review. *International Communications in Heat and Mass Transfer* 76: 6-15. <https://doi.org/10.1016/j.icheatmasstransfer.2016.05.009>
- [7] Lu L, Liu ZH, Xiao HS. (2011). Thermal performance of an open thermosyphon using nanofluids for high-temperature evacuated tubular solar collectors. Part 1: Indoor experiment. *Solar Energy* 85: 379-87. <https://doi.org/10.1016/j.solener.2010.11.008>
- [8] Khanafer K, Vafai K. (2018). A review on the applications of nanofluids in solar energy field. *Renewable Energy* 123: 398-406. <https://doi.org/10.1016/j.renene.2018.01.097>
- [9] Kasaiean A, Sameti M, Daneshazarian R, Noori Z, Adamian A, Ming T. (2018). Heat transfer network for a parabolic through collector as a heat collecting element using nanofluid. *Renewable Energy* 123: 439-49. <https://doi.org/10.1016/j.renene.2018.02.062>
- [10] Bianco V, Scarpa F, Tagliafico LA. (2018). Numerical analysis of the  $\text{Al}_2\text{O}_3$ -water nanofluid forced laminar convection in an asymmetric heated channel for application in flat plate PV/T collector. *Renewable Energy* 116: 9-21. <https://doi.org/10.1016/j.renene.2017.09.067>
- [11] Hawwash AA, Rahman AKA, Nada SA, Ookawara S. (2018). Numerical investigation and experimental verification of performance enhancement of flat plate collector using nanofluid. *Applied Thermal Engineering* 130: 363-74. <https://doi.org/10.1016/j.applthermaleng.2017.11.027>
- [12] Genc AM, Ezan MA, Turgut A. (2018). Thermal performance of a nanofluid-based flat plate solar collector: A transient numerical study. *Applied Thermal Engineering* 130: 305-407. <https://doi.org/10.1016/j.applthermaleng.2017.10.166>
- [13] Ozsoy A, Corumlu V. (2018). Thermal performance of a thermosyphon heat pipe evacuated tube solar collector using silver-water nanofluid for commercial applications. *Renewable Energy* 122: 26-34. <https://doi.org/10.1016/j.renene.2018.01.031>
- [14] Colangelo G, Favale E, Miglietta P, de Risi A, Milanese M, Laforgia D. (2015). Experimental test of an innovative high concentration nanofluid solar collector. *Applied Energy* 154: 874-81. <https://doi.org/10.1016/j.apenergy.2015.05.031>
- [15] Farajzadeh E, Movahed S, Hosseini R. (2018). Experimental and numerical investigations on the effect of  $\text{Al}_2\text{O}_3/\text{TiO}_2\text{-H}_2\text{O}$  nanofluids on thermal efficiency of the flat plate solar collector. *Renewable Energy* 118: 122-30. <https://doi.org/10.1016/j.renene.2017.10.102>
- [16] Kasaiean A, Deshazarian R, Pourfayaz F. (2017). Comparative study of different nanofluids applied in a through collector with glass-glass absorber tube. *Journal of Molecular Liquids* 234: 315-23. <https://doi.org/10.1016/j.molliq.2017.03.096>
- [17] Choi SUS, Zhang ZG, Yu W, Lockwood FE, Grulke EA. (2001). Anomalous thermal conductivity enhancement in nanotube suspensions. *Applied Physics Letters* 79(14): 2252-54. <https://doi.org/10.1063/1.1408272>
- [18] Xuan Y, Roetzel W. (2000). Conceptions for heat transfer correlation of nanofluids. *International Journal*

of Heat Mass Transfer 43(19): 3701-7. <a href="https://doi.org/10.1016/S0017-9310(99)00369-5">https://doi.org/10.1016/S0017-9310(99)00369-5</a>	ETSC	Evacuated tube solar collectors
[19] Kasaeian A, Daviran S, Azarian RD, Rashidi A. (2015). Performance evaluation and nanofluid using capability study of a solar parabolic through collector. Energy Conversion and Management 89: 368-75. <a href="https://doi.org/10.1016/j.enconman.2014.09.056">https://doi.org/10.1016/j.enconman.2014.09.056</a>	K	thermal conductivity, $\text{W m}^{-1} \text{K}^{-1}$
[20] Sakar J. (2011). A critical review on convective heat transfer correlations of nanofluids. Renewable Sustainable Energy Reviews 15(6): 3271-7. <a href="https://doi.org/10.1016/j.rser.2011.04.025">https://doi.org/10.1016/j.rser.2011.04.025</a>	f	Fractional primary energy saving for a solar cooling system
[21] Ghaderian J, Sidik NAC. (2017). An experimental investigation on the effect of $\text{Al}_2\text{O}_3$ /distilled water nanofluid on the energy efficiency of evacuated tube solar collector. International Journal of Heat and Mass Transfer 108: 972-87. <a href="https://doi.org/10.1016/j.ijheatmasstransfer.2016.12.101">https://doi.org/10.1016/j.ijheatmasstransfer.2016.12.101</a>	G	Incident global solar radiation on the collector, $\text{W m}^{-2}$
[22] SketchUp; 2012. <a href="http://www.sketchup.com">http://www.sketchup.com</a> .	m	Volumetric flow rate, $\text{l s}^{-1}$
[23] Fong KF, Chow TT, Lee CK, Lin Z, Chan LS. (2010). Comparative study of different solar cooling system for buildings in subtropical city. Solar Energy 84(2): 227-44. <a href="https://doi.org/10.1016/j.solener.2009.11.002">https://doi.org/10.1016/j.solener.2009.11.002</a>	PEC	Performance evaluation criterion, -
[24] Sparber W, Thuer A, Besana F, Streicher W, Henning HM. (2008). Unified monitoring procedure and performance assessment for solar assisted heating and cooling systems. Presented at EUROSUN 2008.	$Q_{\text{boiler}}$	Heat energy of the auxiliary boiler, kWh
[25] Roy C, Gherasim I, Nadeau F, Poitras G, Nguyen CT. (2012). Heat transfer performance and hydrodynamic behaviour of turbulent nanofluid radial flows. International Journal of Thermal Science 58: 120-9. <a href="https://doi.org/10.1016/j.ijthermalsci.2012.03.009">https://doi.org/10.1016/j.ijthermalsci.2012.03.009</a>	W	Energy of pump, kWh
	$Q_{\text{solar}}$	Heat energy gain from solar collectors, kWh
	$Q_{\text{cooling,ref}}$	Energy cold provided by a conventional system, kWh
	SF	Solar fraction
	$T_{\text{coll,o}}$	Outlet temperature of solar collector, $^{\circ}\text{C}$
	$T_{\text{coll,i}}$	Inlet temperature of solar collector, $^{\circ}\text{C}$
	$T_{\text{st,i}}$	Inlet temperature of hot storage tank, $^{\circ}\text{C}$
	$T_{\text{st,o}}$	Outlet temperature of hot storage tank, $^{\circ}\text{C}$

### Greek symbols

$\eta$	Thermal efficiency of solar collector, -
$\varepsilon_{\text{heat}}$	Efficiency of supplementary boiler, -
$\varepsilon_{\text{cooling}}$	Efficiency of thermal power plant, -
$\phi$	solid volume fraction
$\rho$	Density, $\text{kg m}^{-3}$
$\mu$	dynamic viscosity, $\text{kg m}^{-1}\text{s}^{-1}$
$\Delta T$	Temperature difference between fluid and ambient temperature, $^{\circ}\text{C}$

### Subscripts

bf	Base fluid (water)
p	nanoparticle
w	water
nf	nanofluid

### NOMENCLATURE

$A_c$	Solar collector area, $\text{m}^2$
COP	Coefficient of performance, -
$c_p$	Specific heat, $\text{J kg}^{-1} \text{K}^{-1}$